UNIVERSAL PROPERTIES OF ESCAPE IN DYNAMICAL SYSTEMS

CHRISTOS SIOPIS*, HENRY E. KANDRUP** and G. CONTOPOULOS*
Department of Astronomy, University of Florida, Gainesville, Florida, USA
and
RUDOLF DVORAK
Institut für Astronomie, Universität Wien, Türkenschanzstrasse 17, A-1180 Wien, Austria

Abstract. This paper summarizes a numerical study of the escape properties of three two-dimensional, time-independent potentials possessing different symmetries. It was found, for all three cases, that (i) there is a rather abrupt transition in the behaviour of the late-time probability of escape, when the value of a coupling parameter, ϵ, exceeds a critical value, ϵ_2. For $\epsilon > \epsilon_2$, it was found that (ii) the escape probability manifests an initial convergence towards a nearly time-independent value, $p_0(\epsilon)$, which exhibits a simple scaling that may be universal. However, (iii) at later times the escape probability slowly decays to zero as a power-law function of time. Finally, it was found that (iv) in a statistical sense, orbits that escape from the system at late times tend to have short time Lyapounov exponents which are lower than for orbits that escape at early times.

Key words: Chaotic Phenomena

1. Introduction

The aim of this paper is to review work that has been done in recent years on possibly universal escape properties of two-dimensional time-independent Hamiltonian systems ((Contopoulos, 1990), (Contopoulos and Kaufmann, 1992), (Contopoulos *et al.*, 1993), (Siopis *et al.*, 1995a), (Siopis *et al.*, 1995b)) as well as to report on some of the latest results. Three different systems have been studied, characterized respectively by the following Hamiltonians:

$$\begin{aligned} H_1 &\equiv \frac{1}{2}\left(\dot{x}^2+\dot{y}^2+x^2+y^2\right) - \epsilon x^2y^2 = h_1, \\ H_2 &\equiv \frac{1}{2}\left(\dot{x}^2+\dot{y}^2+x^2+y^2\right) - \epsilon xy^2 = h_2, \\ H_3 &\equiv \frac{1}{2}\left(\dot{x}^2+\dot{y}^2+x^2+y^2-\frac{2}{3}y^3\right) + \epsilon x^2y = h_3. \end{aligned} \tag{1}$$

The first two systems each correspond to two harmonic oscillators, coupled via a quartic or cubic term which is multiplied by a coupling parameter ϵ. The last system is characterized by a modified Hénon-Heiles potential that allows for control of the coupling strength between the two space dimensions via the coupling parameter ϵ. When $\epsilon = 1$, H_3 becomes the standard Hénon-Heiles potential.

The isopotential surfaces that correspond to these Hamiltonians are shown in Figure 1. For a fixed energy h_i, $i = 1,2,3$, no orbit can escape if the value of ϵ is less than a critical $\epsilon_{esc} = \epsilon_{esc}(h_i)$. For $\epsilon \geq \epsilon_{esc}$, the isopotential surfaces

* Also: Astronomy Department, University of Athens, Panepistimiopolis, 157 84 Athens, Greece.
** Also: Department of Physics and Institute for Fundamental Theory, University of Florida.

Celestial Mechanics and Dynamical Astronomy **65**: 57–68, 1997.

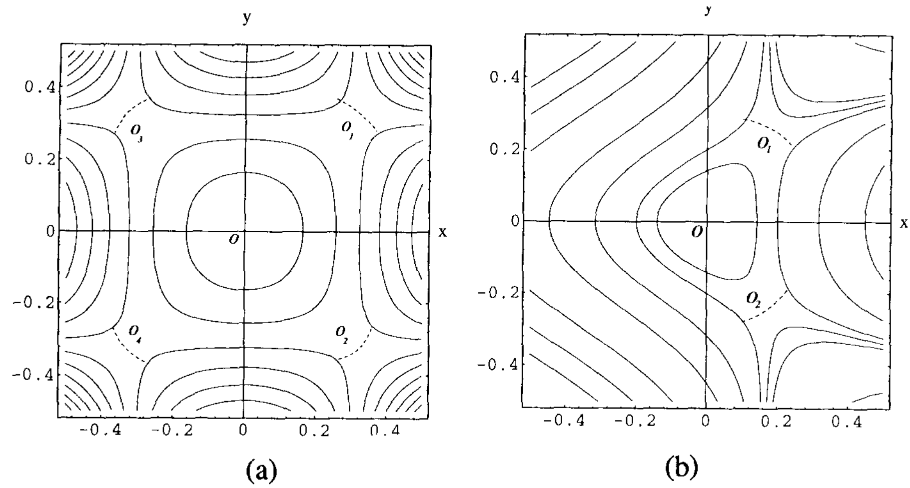

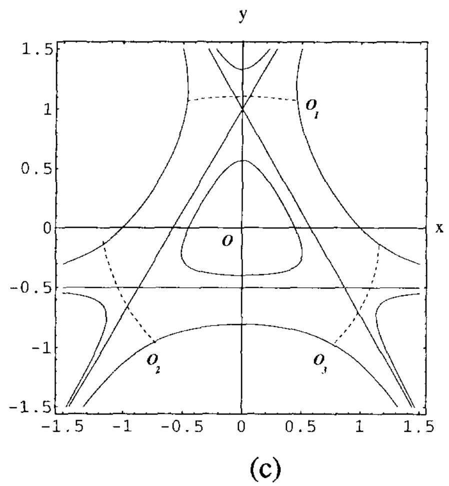

Fig. 1. Equipotential surfaces of the potential that corresponds to (a) H_1 for $\epsilon = 5.26$ and different values of h_1; (b) H_2 for $\epsilon = 3.0$ and different values of h_2; (c) H_3 for $\epsilon = 1.0$ and different values of h_3. O_1, O_2, O_3 and O_4 represent Lyapounov unstable periodic orbits.

form channels of escape, through which orbits can leak out. Any orbit that crosses, moving outward, one of the so-called Lyapounov unstable periodic orbits (see Figure 1), will escape from the system (Churchill *et al.*, 1979).

It will be shown in the following section that the escape properties that were found proved to be the same for all three Hamiltonians, despite their different symmetries. This result suggests strongly that the escape properties depend on generic phase-space characteristics rather than the details of individual potentials, and has motivated the claim for universality.

2. Short-Term Behaviour

The objective here is to study the escape properties of ensembles of orbits moving under the influence of the potentials associated with H_1, H_2 or H_3. To that end, a large number of orbits were computed numerically and followed up to a maximum

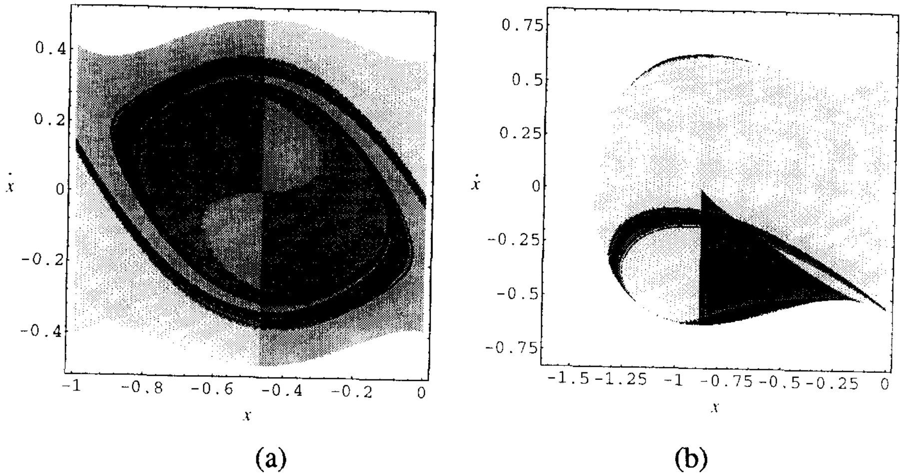

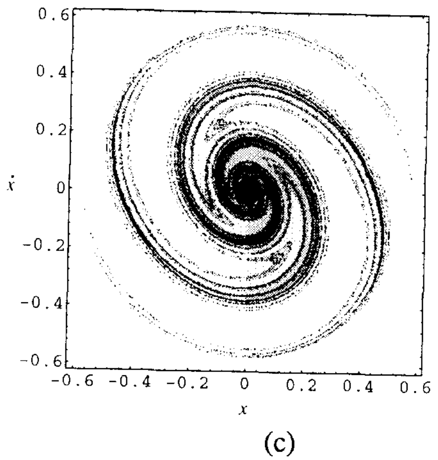

Fig. 2. The plane $(x-\dot{x})$ from which the initial conditions were sampled, for orbits characterized by the Hamiltonian (a) H_1 for $\epsilon = 5.26$; (b) H_2 for $\epsilon = 3.0$; (c) H_3 for $\epsilon = 1.3$. Darker shading implies longer escape times. Resolution is 400×400.

time or until they escaped, whichever happened first. In all experiments, time was discretised in terms of "consequents", defined as the number of intersections of the orbit with the $x = 0$ plane with $\dot{x} < 0$. The initial conditions were chosen to sample uniformly a square in the $(x - \dot{x})$ plane with $y = 0$, and $\dot{y} \geq 0$ uniquely determined from Eqs. (1). Figure 2 uses variable shading to illustrate the dependence of escape time on the initial conditions for the three Hamiltonians considered here. One can see that, whereas escape time is a rather smooth function of initial conditions in certain regions of phase space, elsewhere there is an extremely sensitive dependence on initial conditions. In fact, the latter regions exhibit the nearly self-similar structure characteristic of fractals (see (Contopoulos *et al.*, 1993) for more details).

For each Hamiltonian, ten 0.05×0.05 square cells were chosen to sample some of the "interesting" regions of phase space, *i.e.*, those exhibiting strong fractal structure. Scaling properties of the flow were also examined by studying smaller

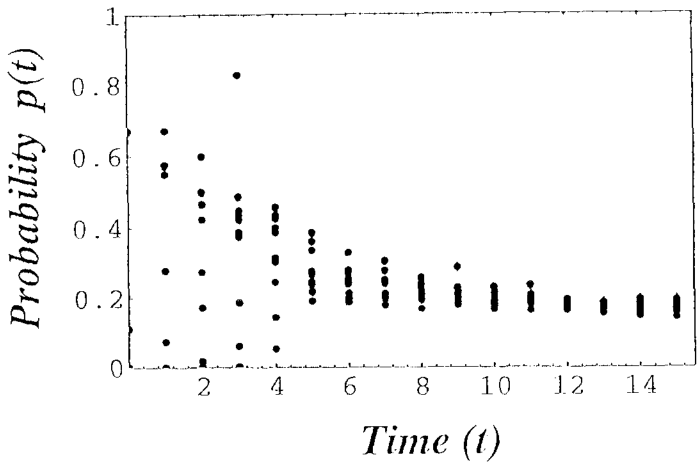

Fig. 3. The escape probability as a function of time for H_3, for $\epsilon = 1.3 > \epsilon_2$ (the error bars are too small compared to the dot size). Results of experiments from ten different cells of initial conditions with size 0.05×0.05 have been superimposed to produce the graph.

phase space regions, in some cases allowing for square cells with sides smaller by a factor of 500. For H_1, the initial $(x, \dot{x})$ pairs were sampled using a grid with an approximate resolution of 200×200 and a time-series orbit integrator. Using a Lie integration scheme (Hanslmeier and Dvorak, 1984) and an improved code to integrate the orbits, resolutions of 400×400, 800×800 and 1600×1600 as well as longer integration times were feasible for H_2 and H_3. The above procedure was repeated for several values of the coupling parameter ϵ.

The basic quantity of interest in this work is the probability $p(\epsilon, t)$ that an orbit will escape at time t from a Hamiltonian system with a coupling parameter ϵ, defined naturally via the relation

$$p(\epsilon, t) \pm \Delta p(\epsilon, t) = \frac{N_{esc} \pm \sqrt{N_{esc}}}{N_{tot}}. \tag{2}$$

Here N_{esc} is the number of trajectories from a given cell that escape between $t-1$ and t, N_{tot} is the total number of trajectories still present at $t-1$, and $\Delta p(\epsilon, t)$ represents an estimate of the uncertainty in the computed escape probability.

For $\epsilon < \epsilon_{esc}$ no orbit can escape and thus $p(\epsilon, t) = 0$ for all times. When $\epsilon \geq \epsilon_{esc}$, it is energetically *possible* for the orbits to escape. However, until a given orbit is actually calculated, it is not known if or when that orbit will escape. The numerical experiments show that, for a fixed energy, some orbits escape relatively fast whereas some others remain in the system for considerably longer times. In fact, slow escapers can remain bound for intervals more than two orders of magnitude longer than fast escapers. The escape probability behaves rather irregularly during the first several crossing times, in a fashion that reflects the specific choice of initial conditions (Figure 3). However, after these initial transients, $p(\epsilon, t)$ tends towards a constant value $p_0(\epsilon)$, the value of which depends on ϵ but not on the choice of the sampling square. More specifically, it appears that there is a critical value $\epsilon_2 > \epsilon_{esc}$ such that for $\epsilon_{esc} \leq \epsilon < \epsilon_2$, $p_0(\epsilon) \equiv 0$, whereas for $\epsilon > \epsilon_2$, $p(\epsilon, t)$ evolves towards a constant, nonzero value, $p_0(\epsilon)$. This transition occurs quite abruptly, within a narrow interval bracketing ϵ_2, and is strongly reminiscent of a phase transition.

It should be noted at this point that, as will be shown in the next section, the probability of escape $p_0(\epsilon)$ in the $\epsilon > \epsilon_2$ regime does *not* actually remain constant. Rather, it decays slowly with time. The rate of decay depends on the particular choice of Hamiltonian, but for the three systems considered here it is slow enough to justify the approximation that $p_0(\epsilon) \approx$ const. at intermediate (not too long) time scales.

The remainder of this section, as well as the following section will investigate properties of escape in the regime where $\epsilon > \epsilon_2$.

For all three Hamiltonians, a simple scaling behaviour was found, involving three distinct quantities ((Contopoulos *et al.*, 1993), (Siopis *et al.*, 1995a),(Siopis *et al.*, 1995b)):

i. the escape probability, $p_0(\epsilon)$;

ii. the time, $T(\epsilon)$, that is required for $p(\epsilon, t)$ to converge towards $p_0(\epsilon)$, for a fixed subset S of phase space volume, from which the initial con 'itions were sampled; and

iii. the time, $T(r)$, that is required for $p(\epsilon, t)$ to converge towards $p_0(\epsilon)$, as a function of the characteristic size r of S, for a fixed value of ϵ.

The following relations characterize the scaling:

$$\begin{aligned} p_0(\epsilon) &\propto (\epsilon - \epsilon_2)^{\alpha}, \\ T(\epsilon) &\propto (\epsilon - \epsilon_2)^{-\beta}, \\ T(r) &\propto r^{-\delta}. \end{aligned} \quad (3)$$

The numerical values of ϵ_2, the exponents α, β and δ as well as other relevant information for the three Hamiltonians can be found in Table I. It is significant that, within statistical uncertainties, the respective exponents of all three Hamiltonians could be identical. Also, again within statistical errors, $\alpha - \beta - \delta = 0$. This is more convincing for H_1 and H_3 than it is for H_2, which may be due to the superposition of short- and long-term behaviour.

3. Long-Term Behaviour

The results presented in the previous section, and in particular the evolution of $p(\epsilon, t)$ towards a constant $p_0(\epsilon)$, were obtained by integrating the orbits for roughly 20 crossing times. Thus, a natural question to ask is whether $p(\epsilon, t)$ remains constant at much later times. In order to address this question, a set of longer simulations were run for the system H_3. The results (Siopis *et al.*, 1995b) show that $p(\epsilon, t)$ is

TABLE I
System parameters of relevance to escape properties.

	H_1	H_2	H_3
h	0.12	0.125	$1/6 \approx 0.167$
ϵ_{esc}	$1/(4h) \approx 2.08$	$1/\sqrt{8h} = 1.00$	1.00
ϵ_2	4.90 ± 0.01	$1.15^{+0.02}_{-0.05}$	1.10 ± 0.05
α	0.49 ± 0.05	0.46 ± 0.05	0.45 ± 0.05
β	$0.39^{+0.14}_{-0.06}$	$0.50^{+0.15}_{-0.10}$	$0.37^{+0.10}_{-0.07}$
δ	0.08 ± 0.03	0.11 ± 0.03	0.12 ± 0.03

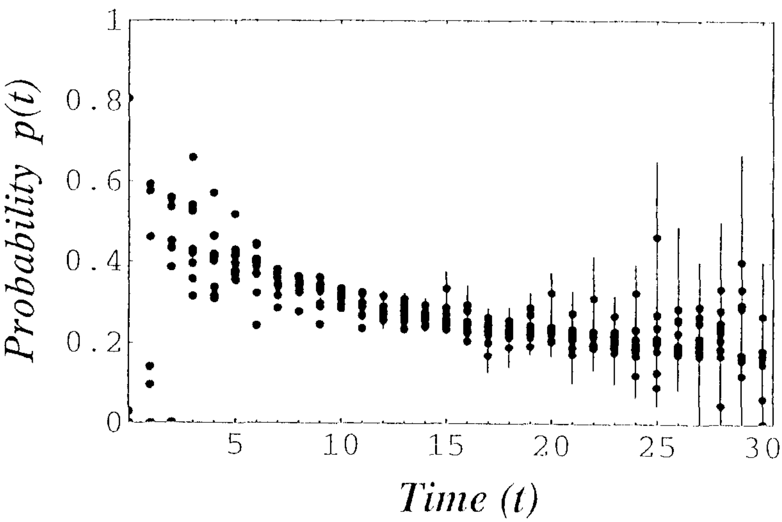

Fig. 4. The long-term decay for the Hamiltonian H_3 and $\epsilon = 1.6$.

not in fact constant. It decays, albeit slowly, with time (Figure 4). The total escape probability at late times was found to be well fit by the empirical relation

$$p(t) \sim t^{-\mu}. \tag{4}$$

Experiments with several values of ϵ indicate that $\mu = 0.31 \pm 0.05$, independent of ϵ.

4. Physical Interpretation

The numerical results obtained in the previous sections can be used to test some simple models of phase-space transport mechanisms. Perhaps the simplest model would be to assume that there is an absolute distinction between two populations of orbits, namely those that can escape and those that cannot. It can then be shown (Contopoulos *et al.*, 1993) that, at late times, $p(t) \propto \exp(-\lambda t)$, where $\lambda = -\ln(1 - p_\infty)$. However, as stated above, the late-time decay scales as a power-law, not exponential, function of time. Therefore, the assumption that there can only be two orbit populations, with no transitions possible between them, does not seem to be a valid one.

An alternative, more plausible, interpretation, can be achieved by invoking the presence of *cantori* around the islands of regularity. It can be shown that modeling of the structure of cantori as self-similar fractals can reproduce the observed late-time power-law decay ((Chirikov and Shepelyansky, 1984), (Hanson *et al.*, 1985), (Bleher *et al.*, 1990)). More specifically, according to the KAM theorem, regular orbits are surrounded in phase space by a hierarchy of invariant topological tori. These KAM tori act as impenetrable barriers that cannot be crossed by orbits, thus segregating phase space into disconnected regions that cannot communicate with each other. However, if somehow the system starts to deviate from integrability, the KAM tori become increasingly convoluted until they eventually lose their integrity and fragment into a Cantor set of holes. Orbits can now leak through these remnants of KAM tori, called cantori ((Contopoulos, 1971), (Aubry and Andre, 1978), (Mather, 1982), (Shirts and Reinhart, 1982)), and diffuse into the surrounding stochastic sea. The diffusion time scale depends on the size of the holes: if the system is sufficiently close to being integrable, the holes are small and diffusion proceeds slowly. However, as deviation from integrability becomes stronger, the holes very rapidly increase in size to the point where they practically no longer impede phase-space transport.

The fragmentation of phase space by KAM tori and cantori leads naturally to the conjecture (*cf.* (Mahon *et al.*, 1995)) that, at any given time, the orbits populating a dynamical system divide approximately into three different classes, namely *regular, sticky* or *temporarily confined chaotic,* and *unconfined chaotic* orbits. The *regular* orbits are trapped forever inside KAM tori. The *sticky*, or *temporarily confined,* orbits can spend a substantial time trapped inside cantori near regular islands, but eventually diffuse through the cantori and find their way out to the stochastic sea. If the phase space were compact, and escape to infinity impossible, the remaining *unconfined chaotic* orbits would simply travel unimpeded throughout the surrounding stochastic sea, although occasionally becoming temporarily confined near the regular islands. Given, however, that escape *is* possible, these orbits will eventually pass through a Lyapounov curve and escape to infinity. (Strictly speaking, in general there will also exist a finite measure of chaotic orbits inside the KAM tori, but these will never be able to enter the surrounding stochastic sea).

The preceding numerical results could then be interpreted if one makes the Ansatz that the transition occurring around ϵ_2 corresponds to the fracture of some dominant KAM tori. In this context, when ϵ exceeds ϵ_2, the last major KAM torus is destroyed, leaving behind one or more cantori which now dominate phase-space transport. Unlike KAM tori, cantori are leaky barriers, and a chaotic orbit moving around inside a cantorus will eventually find its way out in the surrounding stochastic sea through one of the holes of the cantorus. Nevertheless, if the size of the holes is small enough (which is presumably the case for values of ϵ only slightly greater than ϵ_2), an orbit can remain trapped inside the cantorus for extremely long times compared to the natural crossing time ("stickiness" effect). In any case, once in the stochastic sea at large, it will sooner or later escape from the system.

Ensembles of unconfined orbits that populate the stochastic sea inside the Lyapounov curves exhibit a tendency to evolve *towards* a near-invariant distribution (although if the orbits escape or diffuse through the cantori too fast compared to the time scale of approach towards the near-invariant distribution, no real sense of near-invariance may ever be achieved). The unconfined population initially consists only of that subset of the ensemble of initial conditions that lies outside the major cantorus. However, this population is continuously augmented by the orbits that leak through the cantorus. At the same time, orbits are drained from the system as they cross the Lyapounov curves and escape to infinity.

The situation is quite different when $\epsilon < \epsilon_2$. Now a substantial fraction of KAM tori still exist, surrounded by a hierarchy of cantori in the shallows of the stochastic sea. In this case, ensembles of orbits with initial conditions inside the KAM tori are trapped and cannot escape. However, the remaining orbits, even if located initially inside cantori, will eventually escape from the system in a manner similar to the $\epsilon > \epsilon_2$ case described above. In other words, at late times $N_{esc} \to 0$ [see Eq. (2)] but $N_{tot} \to N_{tot}^0 \neq 0$, since N_{tot} is bounded from below by the population of orbits inside the KAM tori that never escape. Therefore, the probability of escape as a function of time decays to zero faster than it does in the $\epsilon > \epsilon_2$ case, and does not exhibit the scaling behaviour observed for $\epsilon > \epsilon_2$ [Eqs. (3)].

5. Escape Time and Short Time Lyapounov Exponents

In the previous section, the distinction was made between three different types of orbits that can populate a dynamical system, namely regular, sticky or temporarily confined chaotic, and unconfined chaotic. This distinction was motivated by the presence of KAM tori and cantori, with the former acting as absolute and the latter as leaky barriers, together determining the dynamics of phase-space transport. Moreover, an interpretation was offered as to how such a model could explain the numerical results, *i.e.*, the initial convergence of the escape probability towards $p_0(\epsilon)$ and the subsequent power-law decay to zero.

An independent tool for gaining insight into phase-space transport and differentiated orbit populations is the (maximal) short time Lyapounov exponent $\chi(\Delta t)$, defined as

$$\chi(\Delta t) = \lim_{\delta z(0)\to 0} \frac{1}{\Delta t} \ln\left(\frac{\| \delta z(\Delta t) \|}{\| \delta z(0) \|}\right),$$

where $\delta z(0)$ is the initial phase-space perturbation and $\|\|$ represents a suitable (*e.g.*, Euclidean) norm (*cf. e.g.* (Grassberger *et al.*, 1988), (Kandrup and Mahon, 1994), (Voglis and Contopoulos, 1994)). This is the finite-time analogue of the well-known asymptotic maximal Lyapounov exponent $\chi \equiv \lim_{\Delta t\to\infty} \chi(\Delta t)$, which is

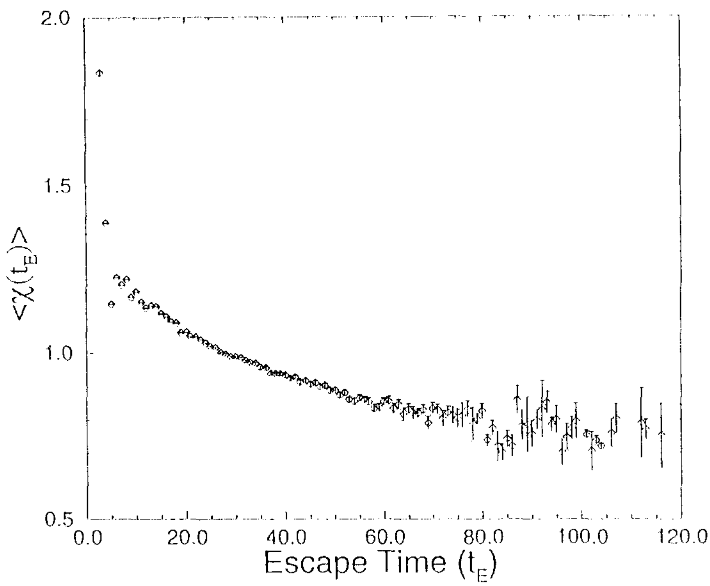

Fig. 5. The average short time Lyapounov exponent $\langle\chi(t_E)\rangle$ for ensembles of orbits that escape at time t_E versus t_E.

a measure, in an asymptotic sense, of the average rate of exponential instability of an orbit.

The usefulness of short time Lyapounov exponents for the problem at hand stems from the following two observations:

- First, one would expect that, for a given time interval Δt_0, the average of the short time Lyapounov exponents $\langle\chi(\Delta t_0)\rangle$ of a randomly chosen ensemble of sticky orbits restricted inside a major cantorus will be *smaller* than the corresponding $\langle\chi(\Delta t_0)\rangle$ of a randomly chosen ensemble of orbits moving around in (but without escaping from) the stochastic sea (*cf.* (Mahon *et al.*, 1995)).
- Second, in the spirit of the discussion of the previous section, the majority of the orbits that escape from the system at early times (say, before $t = 15$ or so) belong to that subset of the initial ensemble of orbits whose initial conditions placed them in the stochastic sea. By contrast, most of the orbits that escape at later times started as sticky orbits inside one of the major cantori wherein they spent most of their time until they crossed the cantorus through one of its holes and entered the stochastic sea, thus becoming unconfined. Escape followed relatively soon thereafter.

With these two observations in mind, one would expect that the average short time Lyapounov exponent for an ensemble of orbits that escape at early times will be *greater* than for an ensemble of orbits that escape at later times. This is so because the later an orbit escapes from the system the more time it will have spent

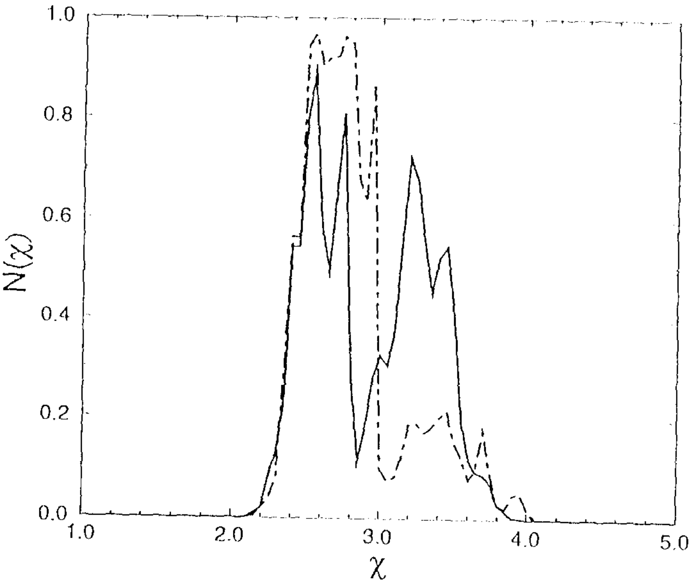

Fig. 6. The distribution $N[\chi(t)])$ at $t = 10$ of the short time Lyapounov exponents of the orbits that escape (i) at $10 \leq t_E < 15$ (solid line) and (ii) at $t_E \geq 40$ (dot-dashed line).

inside the lower-χ environment of a major cantorus relative to the time it spent in the higher-χ environment of the stochastic sea before it escaped. In other words, the lower Lyapounov exponents associated with the region inside the cantorus will weigh more towards the final average short time Lyapounov exponent.

In order to check the validity of this qualitative description, the following numerical experiment was performed. For the Hamiltonian H_3 with $\epsilon = 1.30$, a 0.05×0.05 square of initial conditions was sampled with a resolution of 1000×1000 and the orbits were evolved as in the previous sections until they escaped. In order to compute the short time Lyapounov exponent, a perturbation of magnitude $\| \delta z \| = 10^{-12}$ was introduced in the x coordinate of each orbit at $t = 0$. The perturbation was renormalised each time $\| \delta z \|$ exceeded 10^{-8}. At very early times, the computed exponent will depend sensitively on the initial δz, but for $t > 5$ or so it will provide a reasonable approximation to the exponent in the most unstable direction.

Some of the results are shown in Figures 5 and 6 (a more complete discussion will be presented in a future paper). Figure 5 plots the average short time Lyapounov exponent, $\langle \chi(\Delta t) \rangle = \langle \chi(t_E - 0) \rangle = \langle \chi(t_E) \rangle$, of an ensemble of orbits that escape at a given time t_E as a function of t_E. It is important to emphasize that, for any given escape time along the abscissa, only the Lyapounov exponents of those orbits that escape at that particular time are considered in the average. All the other orbits that are present, but escape at later times, are excluded. It is evident that orbits escaping at later times tend to have short time Lyapounov exponents that are smaller than orbits escaping at early times, in agreement with the interpretation given above.

In order to further test the validity of this simple model, a more detailed dissection of the system was made at a fixed early time. Figure 6 shows the distribution $N[\chi(t)])$ at $t = 10$ of the short time Lyapounov exponents of the orbits that escape (i) at $10 \leq t_E < 15$ (solid line) and (ii) at $t_E \geq 40$ (dot-dashed line). It is obvious that, despite the presence of some structure, there is an overall correlation between the computed χ and the time of escape. Orbits that escape from the system at early times tend systematically to have higher short time Lyapounov exponents than orbits that escape at later times.

Acknowledgements

The authors would like to thank Heinrich Eichhorn for his comments on the statistical interpretation of the numerical data.

H.E.K. was supported in part by the National Science Foundation Grant PHY92-03333. The remaining authors were supported in part by the European Community Human Capital and Mobility Program ERB4050 PL930312 (FWF project 10212-AST).

C.S. would like to thank the Department of Astronomy, the Graduate School and the Graduate Student Council of the University of Florida as well as the Organizing Committee for the financial support.

Some of the computations in this paper were effected using computer time made available through the Research Computing Initiative at the Northeast Regional Data Center (Florida) by arrangement with IBM.

References

S. Aubry and G. Andre. In A. R. Bishop and T. Schneider, editors, *Solitons and Condensed Matter Physics*, Springer Lecture Notes in Physics, Berlin, 1978. Springer.

S. Bleher, C. Grebogi, and E. Ott. *Physica D*, 46:87, 1990.

B. V. Chirikov and D. L. Shepelyansky. *Physica D*, 13:395, 1984.

R. C. Churchill, G. Pecelli, and D. L. Rod. In G. Casati and J. Ford, editors, *Como Conference Proceedings on Stochastic Behavior in Classical and Quantum Hamiltonian Systems*, volume 93 of *Springer Lecture Notes in Physics*, page 76, Berlin, 1979. Springer.

G. Contopoulos. *AJ*, 76:147, 1971.

G. Contopoulos. *Astron. Astrophys.*, 231:41, 1990.

G. Contopoulos and D. E. Kaufmann. *Astron. Astrophys.*, 253:359, 1992.

G. Contopoulos, H. E. Kandrup, and D. E. Kaufmann. *Physica D*, 64:310, 1993.

P. Grassberger, R. Badii, and A. Poloti. *J. Stat. Phys.*, 51:135, 1988.

A. Hanslmeier and R. Dvorak. *Astron. Astrophys.*, 132:203, 1984.

J. D. Hanson, J. R. Cary, and J. D. Meiss. *J. Stat. Phys.*, 39:327, 1985.

H. E. Kandrup and M. E. Mahon. *Astron. Astrophys.*, 290:762, 1994.

M. E. Mahon, R. A. Abernathy, Bradley B. O., and H. E. Kandrup. *Mon. Not. R. Astron. Soc.*, 275:443, 1995.

J. N. Mather. *Topology*, 21:457, 1982.

R. S. Shirts and W. P. Reinhart. *J. Chem. Pjus.*, 77:5204, 1982.

C. V. Siopis, G. Contopoulos, and H. E. Kandrup. In H. E. Kandrup, S. T. Gottesman, and J. R. Ipser, editors, *Three-Dimensional Systems*, volume 751 of *Annals of the New York Academy of Sciences*, pages 205–212, 1995.

C. V. Siopis, G. Contopoulos, H. E. Kandrup, and R. Dvorak. In J. H. Hunter, R. E. Wilson, and J. R. Ipser, editors, *Waves in Astrophysics*, volume 773 of *Annals of the New York Academy of Sciences*, pages 221–230, 1995.

N. Voglis and G. Contopoulos. *J. Phys. A*, 27:4899, 1994.